Hole doping in $BaFe_2As_2$: The case of $Ba_{1-x}Na_xFe_2As_2$ single crystals

S. Aswartham, M. Abdel-Hafiez, D. Bombor, M. Kumar, A. U. B. Wolter, C. Hess, D. V. Evtushinsky, V. B. Zabolotnyy, A. A. Kordyuk, T. K. Kim,* S. V. Borisenko, G. Behr, B. Büchner, and S. Wurmehl†
Leibniz Institute for Solid State and Materials Research, IFW, D-01069 Dresden, Germany
(Received 29 February 2012; revised manuscript received 4 June 2012; published 15 June 2012)

Single crystals of $Ba_{1-x}Na_xFe_2As_2$ with $x = 0, 0.25, 0.35, 0.4$ were grown using a self-flux high temperature solution growth technique. The superconducting and normal state properties were studied by temperature dependent magnetic susceptibility, electrical resistivity, and specific heat, revealing that the magnetic and structural transition is rapidly suppressed upon Na substitution at the Ba site in $BaFe_2As_2$, giving rise to superconductivity. A superconducting transition as high as 34 K is reached for a Na content of $x = 0.4$. The positive Hall coefficient confirms that the substitution of Ba by Na results in hole doping similar to the substitution of Ba by K. Angle resolved photoemission spectroscopy was performed on all $Ba_{1-x}Na_xFe_2As_2$ crystals. The Fermi surface of hole-doped $Ba_{1-x}Na_xFe_2As_2$ is to a large extent the same as the Fermi surface found for the K-doped sister compounds, suggesting a similar impact of the substitution of Ba by either K or Na on the electronic band dispersion at the Fermi level.

DOI: 10.1103/PhysRevB.85.224520 PACS number(s): 74.70.Xa, 74.62.Bf, 74.25.Jb, 74.25.F−

I. INTRODUCTION

The recent discovery of superconductivity in $LaO_{1-x}F_xFeAs$ with critical temperatures up to 26 K (Ref. 1) has significantly increased research activities in the field of superconductivity. After the first report on pnictide superconductors, the critical transition temperature T_c has been enhanced to 55 K in $SmO_{1-x}F_xFeAs$.[2] The availability of different types of materials in this new family of superconductors allows addressing many open questions in superconductivity, e.g., the question as to whether magnetism and superconductivity are coexisting or competing. The Fe-based superconductors are classified into four main types according to their stoichiometry, such as the series of 1111 (*R*OFeAs and *AE*FFeAs with *R* a rare earth, and *AE* an alkali earth metal),[1,3] 122 (*AE*Fe_2As_2 and AFe_2As_2 with *AE* an alkaline earth metal, and *A* an alkali),[4,5] 111 (*A*FeAs),[6] and 11 ($FeSe_{1-x}Te_x$).[7] Although the T_c of the 1111 family is found to be the highest among the Fe-based superconductors, their intrinsic properties need to be explored. For instance, the detailed electronic structure still needs to be investigated, primarily due to the challenging requirements posed by the high pressure growth technique and, hence, due to the lack of large single crystals.[8] Crystals of the 122 series are comparably easier to grow at ambient pressure and are more convenient to handle than, e.g., the 111 compounds. Therefore the 122 compounds are the best studied pnictide superconductors.

One of the first publications on 122 compounds dates back to 1964.[9] Since then more than 700 compounds have been found to adopt the 122 structure type.[10] All members of the 122 family have the $ThCr_2Si_2$ structure type and are sensitive to chemical substitutions and pressure (see, e.g., Ref. 11). Usually, the parent compound is an antiferromagnet with spin density wave ordering in orthorhombic symmetry. Superconductivity can be achieved either by external pressure or by chemical substitution, which leads to a tetragonal symmetry and suppression of the magnetic ordering. Rotter *et al*. reported superconductivity in K-doped $BaFe_2As_2$ with the highest T_c of 38 K in the 122 series.[4] However, the quest for new superconducting materials continues and many new superconducting materials with different critical temperatures have been synthesized within the 122 series. The report on superconductivity in polycrystalline samples of Na-doped $BaFe_2As_2$ by Cortes-Gil *et al*. can be considered as a recent example.[12] Although this study on polycrystals suggests that $Ba_{1-x}Na_xFe_2As_2$ is quite similar to the corresponding K-substituted sister compounds, a detailed study of the physical properties is lacking in Ref. 12 and in particular single crystals need to be studied. It is, however, necessary to investigate in detail how physical properties vary with different dopants and doping levels, considering the fact that also the electronic structure is significantly modified depending on the nature of the doping elements and the amount of doping. Here, extending the previous work, we report on the growth of $Ba_{1-x}Na_xFe_2As_2$ single crystals with $x = 0$, 0.25, 0.35, 0.4 and on their magnetic, electronic transport, thermodynamic, and electronic properties.

II. MATERIALS AND METHODS

All preparation steps such as weighing, mixing, grinding, and storage were carried out in an Ar-filled glove box (O_2 and H_2O levels of less than 0.1 ppm). All precursor materials were prepared by reacting with As, yielding, e.g., BaAs, FeAs, and Fe_2As. These precursor materials were used for the crystal growth. According to the desired stoichiometry $(Ba_{1-x}Na_x)$:Fe:As were used in a molar ratio of 1:4:4. The corresponding Na was used in its metallic form and was placed at the bottom of the alumina crucible, while the well ground mixture of the prereacted pnictide material was carefully placed on top. The alumina crucible was then put into a niobium container which was sealed under 0.5 atm pressure of argon in an arc-melting facility. The sealed niobium crucible assembly was placed in a vertical furnace with Ar atmosphere. The furnace was heated up to 1373 K at a rate of 100 K/h where it remained for 10 h to ensure homogenous

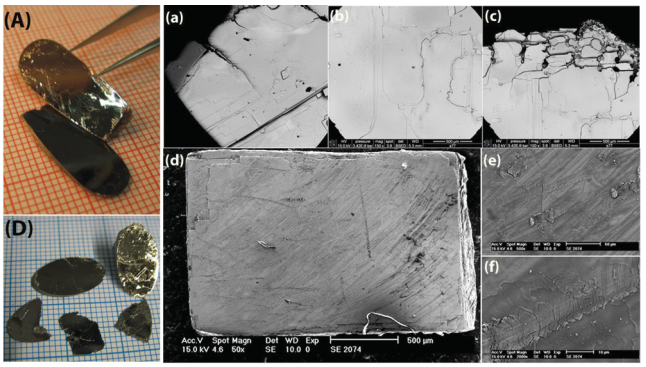

FIG. 1. (Color online) (A) Platelike as-grown single crystals of $Ba_{0.75}Na_{0.25}Fe_2As_2$ from self-flux, (a)–(c) SEM pictures from the same batch of a $Ba_{0.75}Na_{0.25}Fe_2As_2$ single crystal. (D) Platelike as-grown single crystals of $Ba_{0.65}Na_{0.35}Fe_2As_2$. (d)–(e) SEM pictures from the same batch of a $Ba_{0.65}Na_{0.35}Fe_2As_2$ single crystal which shows the typical layer by layer growth.

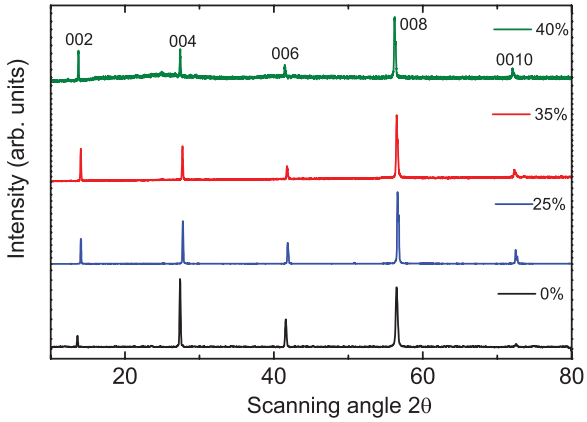

FIG. 2. (Color online) XRD pattern of $Ba_{1-x}Na_xFe_2As_2$ showing only 00*l* reflections. The XRD data were collected using the platelike crystals.

melting and afterward cooled down to 1023 K at a rate of 2 K/h. Finally the furnace was cooled to room temperature at 300 K/h. Plateletlike single crystals of cm size were obtained as demonstrated by Figs. 1(A) and 1(D). The surfaces of the crystals are shiny and metalliclike [see Figs. 1(A) and 1(D)]. All crystals show a layered morphology [Figs. 1(c) and 1(d)]. Typically, they are easy to cleave along the *ab* plane. These cleaving planes are shown in Figs. 1(b) and 1(e).

The quality of the grown single crystals was investigated by complementary techniques. Several samples were examined with a scanning electron microscope (SEM Philips XL 30) equipped with an electron microprobe analyzer for semi-quantitative elemental analysis using the energy dispersive x-ray (EDX) mode. In order to assess the quality of the crystals the homogenous distribution of the Na substituent is highly relevant. Here, the standard deviation (SD) of the average Na composition allows to judge upon the homogeneity of Na within the crystals. Therefore, the composition and in particular the Na-doping level was obtained by averaging over several different points of each single crystal. The corresponding compositions and standard deviations are $x = 0.250 \pm 0.005$, $x = 0.350 \pm 0.01$, and $x = 0.400 \pm 0.01$. The homogenous distribution of Na, as reflected by the small SD, confirms the high homogeneity of our crystals. Figures 1(a)–1(f) exemplarily show the SEM images of the single crystals with Na contents of $x = 0.25$ and $x = 0.35$. The layer by layer growth can be easily seen here.

Figure 2 shows an x-ray diffraction (XRD) pattern taken on platelike single crystals with different Na contents using a Rigaku miniflex with Cu K_α radiation. Only reflections with 00*l* Miller indices are observed, as expected for *c*-axis orientation. All the reflections are indexed based on the $ThCr_2Si_2$ structure type, which confirms the phase purity of our $Ba_{1-x}Na_xFe_2As_2$ single crystals.

Temperature dependent electronic transport was measured using a standard four-probe alternating current dc method with the current applied parallel to the *ab* plane. Electrical contacts parallel to the *ab* plane were made using thin copper wires attached to the sample with silver epoxy.

Magnetization measurements were performed using either the magnetic properties measurement system (MPMS) or the vibrating sample magnetometer (VSM) from Quantum Design. A physical property measurement system (PPMS) with magnetic fields up to 9 T was used to perform the specific heat measurements. During the heat capacity measurements, the sample was cooled to the lowest temperature with an applied magnetic field [field cooled (FC)] and the specific heat data were collected between 1.8 and 200 K (upon warming) by using the relaxation time method. Photoemission experiments for this study have been carried out using synchrotron radiation from the BESSY storage ring at the "1-cubed ARPES" (angle-resolved photoemission spectroscopy) station equipped with a ^{3}He cryostat. Each sample was cleaved directly in the UHV and it was ensured that the samples exhibited a mirrorlike surface before the spectra were recorded.

III. RESULTS AND DISCUSSION

A. Magnetic measurements

Magnetization measurements have been performed after cooling the samples in zero [zero field cooled (ZFC)] and applied (FC) magnetic fields from far above the critical temperature. Figure 3(a) shows the molar susceptibility (χ_{mol}) measured in an applied magnetic field of 1 T with $H \parallel ab$. The susceptibility data of the parent compound clearly shows an anomaly at 137 K which corresponds to the combined structural (T_s) and magnetic (T_{SDW}) transition in $BaFe_2As_2$ (see, e.g., Ref. 13). This transition is clearly suppressed and shifted to lower temperatures upon the substitution of Ba by Na. Specifically, the T_s/T_{SDW} transition for $Ba_{0.75}Na_{0.25}Fe_2As_2$ occurs at 123 K. Moreover, this transition is also significantly broadened compared to the parent compound. The shift and broadening of the T_s/T_{SDW} transition is more apparent in the derivative of the static susceptibility [inset of Fig. 3(a)]. No indication of splitting of the structural and magnetic transition is observed. However, in case of a hole-doped $Ba_{0.86}K_{0.14}Fe_2As_2$ crystal in the underdoped regime grown from Sn flux, a clear splitting of T_s and T_{SDW}, monitored by distinct anomalies in both $d\rho/dT$ and specific heat, was reported by Urbano *et al.*[14] In contrast to that Avci *et al.*

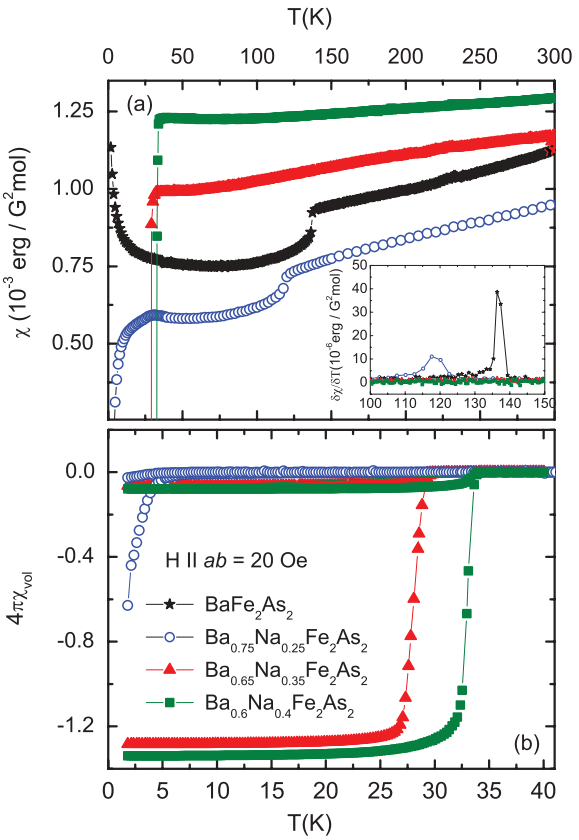

FIG. 3. (Color online) (a) Susceptibility $\chi = M/B$ for $Ba_{1-x}Na_xFe_2As_2$ for different doping levels at $H \parallel ab = 1$ T. The inset shows the derivative of the static susceptibility. (b) Temperature dependence of the volume susceptibility χ_{vol} following the ZFC-FC protocol as described in the text. All data have been collected for $B \parallel ab$ and the applied field was 20 Oe.

found no splitting at all doping levels of polycrystalline $Ba_{1-x}K_xFe_2As_2$ where T_s and T_{SDW} coexist.[15] Generally, samples grown from self-flux are considered to have a higher quality than those grown from Sn flux. As an example, Mathieu *et al.* could show that Sn may even substitute Ba in $BaFe_2As_2$.[16] Such a difference in quality related to the different flux types might explain the absence or presence of the T_s and T_{SDW} splitting. At $T = 10$ K, $Ba_{0.75}Na_{0.25}Fe_2As_2$ undergoes also a superconducting transition, which is a general feature of underdoped samples. Samples with higher Na contents ($x = 0.35, 0.4$) show no indication of either a structural or a magnetic transition, but a superconducting transition only.

Interestingly, all samples show a linear temperature dependence of the susceptibility $\chi(T)$ (see Fig. 3). The range of this linearity is from 300 to about 150 K for samples exhibiting a structural and magnetic transition ($x = 0, 0.25$) and 300–50 K for samples with $x = 0.35, 0.4$. This linearity of the susceptibility has already been discussed for undoped $BaFe_2As_2$ and for both electron-doped $LaO_{1-x}F_xFeAs$ and $Ca(Fe_{1-x}Co_x)_2As_2$.[17,18] So it was concluded that this linearity is a general feature and that the normal state susceptibility is not affected by the type of charge carriers. In the following, we will analyze the slope of the linear part of the magnetic susceptibility. The average slope of the susceptibility $d\chi/dT$ at high temperature is 8×10^{-7} erg/(G^2 mol K), which is similar to the value of the slope reported for the electron-doped $LaO_{1-x}F_xFeAs$ and $Ca(Fe_{1-x}Co_x)_2As_2$.[17] However, the slope of the parent and underdoped compound is very similar [1×10^{-7} erg/(G^2 mol K)] and decreases significantly for the samples with higher Na contents [8×10^{-7} erg/(G^2 mol K) for $x = 0.35$; 3×10^{-7} erg/(G^2 mol K) for $x = 0.4$]. One may conclude that the linearity in susceptibility is a characteristic property of Fe-based superconductors, but that the slope might differ for different types of charge carriers.

Figure 3(b) presents the temperature dependent volume susceptibility (χ_{vol}). χ has been deduced from the measured magnetization and is not corrected for demagnetization effects. The sharp superconducting transition with a transition width of less than 2.5 K confirms the good quality of our crystals. We determine T_c from the bifurcation point between the ZFC and FC magnetization. Using this approach, we estimate T_c to be 10, 29, and 34 K for samples with $x = 0.25$, 0.35, and 0.4, respectively. The critical temperature of our single crystals is in good agreement with the ones observed for polycrystalline samples of Na-doped $BaFe_2As_2$ by Cortes-Gil *et al.*[12]

B. Electronic transport

1. Resistivity

Figure 4 shows the resistivity of all $Ba_{1-x}Na_xFe_2As_2$ single crystals. For the undoped and $x = 0.25$ samples the resistivity shows a sharp drop while the derivative of the resistivity (the inset of Fig. 4) shows a clear maximum at $T(x = 0) = 137$ K and $T(x = 0.25) = 117$ K, typically found in hole-doped 122 compounds (see, e.g., Ref. 19), which is an indication of the structural and magnetic transition. Note that we did not see any indication of a doping induced splitting of this transition as observed in electron-doped 122 compounds.[13,20,21] The normal state resistivity decreases by 20% with doping, which is also observed in K-doped Ba122 compounds[19] in contrast to a decrease of 50% for electron-doped samples.[13,20,21] The sample with ($x = 0.25$) shows both an antiferromagnetic and a superconducting transition which is typically seen in all underdoped 122 compounds.[13,22,23] In general, a transition toward superconductivity could be observed in all samples containing Na. The critical temperature was assigned where

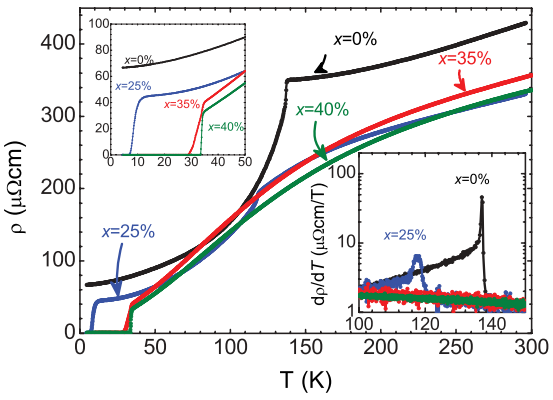

FIG. 4. (Color online) In-plane electronic resistivity ρ of $Ba_{1-x}Na_xFe_2As_2$ single crystals for different Na contents x in dependence of the temperature. Inset: Derivative $d\rho/dT$ around the combined structural and magnetic transition.

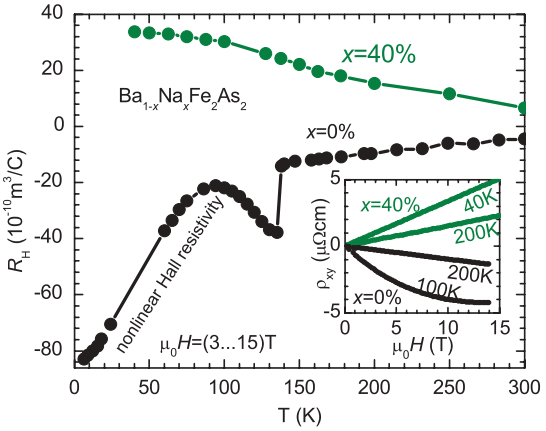

FIG. 5. (Color online) Hall coefficient R_H of optimally doped $Ba_{0.6}Na_{0.4}Fe_2As_2$ and undoped compound in dependence of temperature. Inset: Hall resistivity in dependence of applied magnetic field $\mu_0 H$ for both samples at different temperatures. R_H was determined from the average slope $\rho_{x,y}$ between 3 and 15 T.

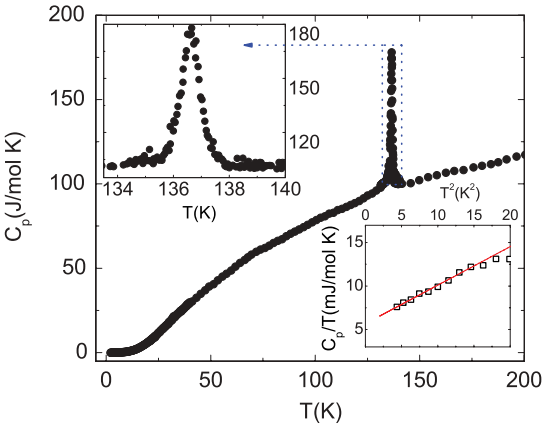

FIG. 6. (Color online) Temperature dependence of the heat capacity measurement on a single crystal of the pristine $BaFe_2As_2$. The combined structural and magnetic transition is clearly seen at 137 K. The upper inset shows the vicinity of the phase transition on an enlarged scale, while the lower inset shows a linear fit to the data in the temperature range between 4 and 20 K.

the resistivity drops to 50% of its value in a normal state. Using this approach, superconductivity is found below $T_c(x = 0.25) = 9$ K, $T_c(x = 0.35) = 32$ K, and $T_c(x = 0.40) = 34$ K, which is in line with the T_c derived from magnetization measurements.

2. *Hall effect*

The Hall effect was measured for the parent and optimally doped compounds ($x = 0,0.4$) by using the same technique as for the resistivity measurement but with the Hall contacts attached. The magnetic field was applied perpendicular to the *ab* plane while the current was passed along the *ab* plane. In order to eliminate any offset of the measured Hall resistivity due to a finite misalignment of the Hall contacts, the Hall resistivity was calculated by using the difference of measurements in positive and negative applied magnetic field. The Hall coefficient R_H of the undoped compound is negative in the whole temperature range (see Fig. 5) and shows a linear decrease with decreasing temperature in the paramagnetic state. At the combined structural and magnetic transition (137 K), the Hall coefficient shows a jumplike behavior and a strong nonlinear temperature dependence in the antiferromagnetic regime. In contrast to this, the optimally doped compound with $x = 0.4$ exhibits a positive Hall coefficient over the full temperature range with a linear increase with decreasing temperature. A similar behavior was observed for the K-doped 122 sister compound, and the positive Hall coefficient is consistent with hole doping upon the substitution of Ba by K or, in the present case, by Na.

C. Specific heat capacity C_p

Figure 6 shows the temperature dependence of the heat capacity for a $BaFe_2As_2$ single crystal. The combined structural and magnetic transition occurs at 137 K, with a rather sharp transition corresponding to a specific heat jump of $\Delta C \sim 98$ J/mol K (see the upper inset of Fig. 6). This transition is sharper than previously reported for $BaFe_2As_2$ by, e.g., Refs. 24–26, and indicates the high quality of our crystals (full width at half maximum ~0.6 K). The transition temperature measured by specific heat is in a good agreement with magnetization and transport (see Secs. III B 1 and III A) and with earlier reports (see, e.g., Refs. 24 and 26). The

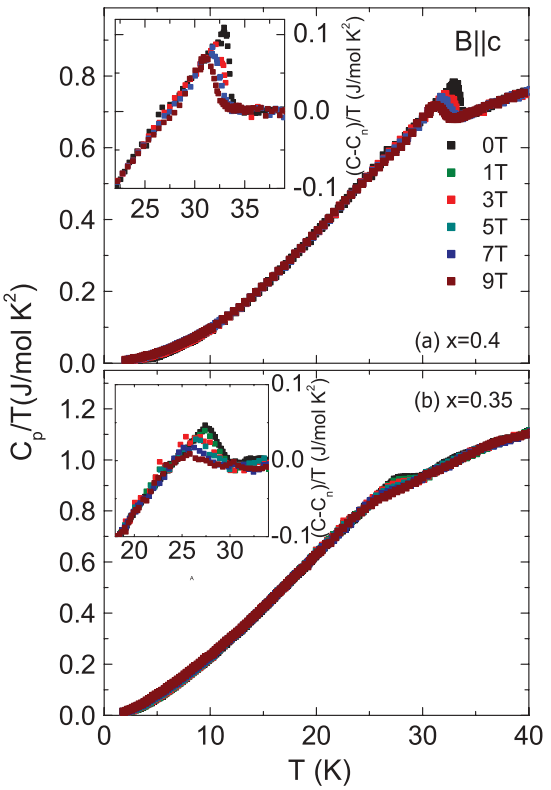

FIG. 7. (Color online) The temperature dependent specific heat of (a) $Ba_{0.6}Na_{0.4}Fe_2As_2$ (b) $Ba_{0.65}Na_{0.35}Fe_2As_2$ in various applied magnetic fields up to 9 T parallel to the c-axis. The insets show a zoom into the superconducting state for both single crystals.

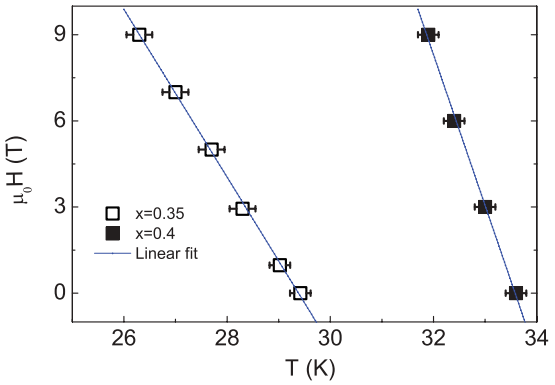

FIG. 8. (Color online) Magnetic phase diagram for $x = 0.35$ and 0.40. The blue dotted line represents a linear fit to the data.

analysis of the data yields a Sommerfeld coefficient γ of 6.13(8) mJ/mol K^2 and a Debye temperature of $\Theta_D = 297$ K, which are comparable with those reported by Sefat *et al.*[25]

Figure 7 shows the temperature dependent specific heat measurements for $Ba_{0.6}Na_{0.4}Fe_2As_2$ [Fig. 7(a)] and $Ba_{0.65}Na_{0.35}Fe_2As_2$ [Fig. 7(b)] single crystals. The measurements prove the bulk nature of superconductivity with a sharp specific heat jump at the superconducting transition temperature $T_c = 29$ K and $T_c = 34$ K for $x = 0.35$ and 0.4, respectively. The critical temperatures as derived from the specific heat data (see below) are in agreement with the T_c found by resistivity and magnetization measurements (see Secs. III A and III B1). The inset of Fig. 7(a) shows the superconducting state of the $x = 0.4$ crystal in different magnetic fields with B parallel to the c axis. Note that these curves were obtained after subtracting the electronic C_{el} and phononic C_{ph} contribution to the specific heat following Eq. (1) (see Ref. 27):

$$C_n = C_{el} + C_{ph} = \gamma T + \beta T^3 + \eta T^5. \quad (1)$$

At low temperatures, i.e., the specific heat is described by the sum of both contributions $C_n = C_{el} + C_{ph} = \gamma T + \beta T^3$, however, the term ηT^5 may be added to improve the fit at higher temperatures. Using Eq. (1) to subtract the electronic C_{el} and phononic C_{ph} contribution to the specific heat, the specific heat jump of the zero-field measurements $\Delta C/T_c$ near the transition is found to be ∼102 mJ/mol K^2 for the $x = 0.4$ sample. Our $\Delta C/T_c$ value is comparable to the $\Delta C/T_c$ reported for a single crystal of the sister compound $Ba_{0.6}K_{0.4}Fe_2As_2$.[28] $\Delta C/T_c$ for the $x = 0.35$ sample amounts to ∼73 mJ/mol K^2. The universal parameter is $\Delta C/\gamma_n T_c = 1.62$ for the $x = 0.4$ sample with $\gamma_n = 62.7$ mJ/mol K^2. This value is comparable to 1.55 reported by Mu *et al.* for the K-doped sister compound $Ba_{0.6}K_{0.4}Fe_2As_2$.[29] $\Delta C/\gamma_n T_c$ is found to be = 1.26 for the $x = 0.35$ sample. Further details about the specific heat jump in $Ba_{0.65}Na_{0.35}Fe_2As_2$ and about the superconducting gap properties are reported in Ref. 30.

Next, we will explore the magnetic phase diagram for the superconducting samples with $x = 0.35, 0.40$. Upon applying various fields with $B \parallel c$, the superconducting transition is systematically shifted to a lower temperature by about 1.5 K, is reduced in height, and is broadened, as shown in the insets of Figs. 7(a) and 7(b).

The exact value of the transition temperature T_c is determined by using an ´entropy conserving construction´ for each field.[31] To extract the upper critical field $H_{c2}(0)$ we used the single-band Werthamer-Helfand-Hohenberg (WHH) model[32] $H_{c2}(0) = -0.69T_c(dH_{c2}/dT)_{T_c}$, as shown by the blue dotted line in Fig. 8. The magnetic phase diagram of both samples is perfectly described by a linear fit with average slopes of $-(dH_{c2}/dT)_{T_c} = 3.3$ T/K and $-(dH_{c2}/dT)_{T_c} = 5.25$ T/K for $x = 0.35$ and 0.40, respectively. From these values, the upper critical field $H^c_{c2}(0)$ is found to be 66 and 121 T for $x = 0.35$ and 0.40, respectively. The value for the upper critical field of the $x = 0.4$ compound is comparable with the critical field reported for $Ba_{0.6}K_{0.4}Fe_2As_2$.[28] In summary, our specific heat analysis underlines the

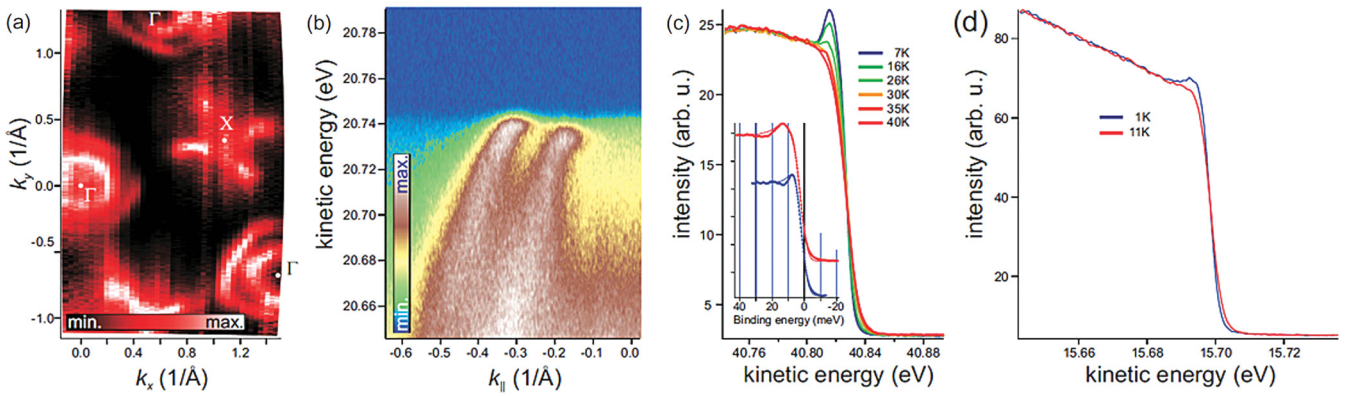

FIG. 9. (Color online) (a) Fermi surface (FS) map, recorded at 80 eV excitation energy from the $Ba_{1-x}Na_xFe_2As_2$ samples with $x = 0.35$ ($T_c = 29$ K). The photoemission intensity distribution was integrated within ±7 meV around the Fermi level. (b) An energy-momentum cut, passing through the Γ point and imaging the inner and outer Γ barrels, recorded at $T = 1$ K for the sample with $x = 0.4$ ($T_c = 34$ K). A smaller superconducting gap can be observed for the outer Γ barrel and a larger one for the inner Γ barrel. (c) Temperature dependence of the density of states, related to the inner Γ barrel, recorded for the sample with $x = 0.4$. Inset: Density of states for outer and inner Γ barrels at 7 K, fitted to the Dynes function (Ref. 33). The determined values for the superconducting gap are 3 ± 0.5 and 10.5 ± 1 meV. (d) Density of states for the inner Γ barrel, recorded at 1 and 11 K for the underdoped sample with $x = 0.25$ ($T_c = 10$ K). The value of the superconducting gap, estimated from the fit, is 1.9 ± 0.5 meV.

similarities of the Na-doped compounds to the K-doped sister compounds.

D. ARPES

Angle-resolved photoemission spectroscopy (ARPES) measurements were carried out on freshly cleaved surfaces of $Ba_{1-x}Na_xFe_2As_2$ samples with $x = 0.25, 0.35, 0.4$. Figure 9(a) exemplarily shows a typical photoemission intensity distribution at the Fermi level, a so-called Fermi surface (FS) map, of the $Ba_{1-x}Na_xFe_2As_2$ sample with $x = 0.35$. In general, the FS of all $Ba_{1-x}Na_xFe_2As_2$ samples consists of holelike sheets at the center of the Brillouin zone (BZ) (Γ point), and of a propellerlike structure at the BZ corner (X point) with holelike propeller blades and small electronlike FS sheets in the center. Thus, the FS of Na-substituted $BaFe_2As_2$ is to a large extent the same as the FS found for K-substituted $BaFe_2As_2$,[33,34] suggesting that the substitution of Ba by either Na or K affects the electronic band dispersion at the Fermi level in a very similar way.

An energy-momentum cut, passing through the Γ point [see Fig. 9(b)], reveals not only well-defined band dispersions for the inner and outer Γ barrels, but also a superconducting gap with a larger magnitude for the inner barrels and with a smaller magnitude for the outer one. The analysis of the temperature dependence of the electronic spectrum of the sample with $x = 0.4$ ($T_c = 34$ K) for different locations in the momentum space [see Fig. 9(c)] allows us to conclude that the superconducting gap distribution is very close to the one observed for the optimally doped $Ba_{1-x}K_xFe_2As_2$:[33] The gap magnitude maximizes for the inner Γ barrel (around 10.5 meV) and minimizes for the outer Γ barrel (around 3 meV). For the underdoped sample with $x = 0.25$ ($T_c = 10$ K) the opening of the superconducting gap was also monitored by the growth of the coherence peak in the density of states below T_c [Fig. 9(d)]. The estimated gap value for the inner Γ barrel in this case is around 2 meV.

IV. CONCLUSIONS AND SUMMARY

In summary, single crystals of $Ba_{1-x}Na_xFe_2As_2$ with $x = 0$, 0.25, 0.35, 0.40 were grown using a self-flux method. The superconducting and normal state properties have been systematically studied by means of temperature dependent magnetic susceptibility, electrical resistivity, Hall cofficients (R_H), and specific heat measurements. Substitution of Ba by Na leads to the suppression of SDW ordering and induces superconductivity up to 34 K for $x = 0.4$. The positive Hall coefficient of $Ba_{0.6}Na_{0.4}Fe_2As_2$ confirms that Na substitution results in hole doping similar to K doping in $Ba_{1-x}K_xFe_2As_2$. Even though the properties of our single crystals do not differ from the previously reported polycrystals, we open a way to study also the electronic structure of another type of hole-doped $BaFe_2As_2$. The investigation of the electronic structure of our $Ba_{1-x}Na_xFe_2As_2$ single crystals by ARPES reveals striking similarities in the Fermi surface with the famous K- (hole-) doped sister compounds. Our results suggest a generic behavior of the 122 series upon hole doping.

ACKNOWLEDGMENTS

The authors thank M. Deutschmann, S. Pichl, and S. Gass for technical support. Work was supported by the Deutsche Forschungsgemeinschaft DFG through the Priority Programme SPP1458 (Grants No. BE1749/13 and No. GR3330/2). S.W. acknowledges support by DFG under the Emmy-Noether programme (Grant No. WU595/3-1).

*Present address: Diamond Light Source Ltd., Didcot OX11 0DE, United Kingdom.

†s.wurmehl@ifw-dresden.de

[1] Y. Kamihara, T. Watanabe, M. Hirano, and H. Hosono, J. Am. Chem. Soc. **130**, 3296 (2008).

[2] Z. A. Ren, W. Lu, J. Yang, W. Yi, X.-L. Shen, Z. C. Li, G. C. Che, X. L. Dong, L. L. Sun, F. Zhou *et al.*, Chin. Phys. Lett. **25**, 2215 (2008).

[3] M. Tegel, S. Johansson, V. Weiss, I. Schellenberg, W. Hermes, R. Pöttgen, and D. Johrendt, Europhys. Lett. **84**, 67007 (2008).

[4] M. Rotter, M. Tegel, and D. Johrendt, Phys. Rev. Lett. **101**, 107006 (2008).

[5] K. Sasmal, B. Lv, B. Lorenz, A. M. Guloy, F. Chen, Y.-Y. Xue, and C.-W. Chu, Phys. Rev. Lett. **101**, 107007 (2008).

[6] J. H. Tapp, Z. Tang, B. Lv, K. Sasmal, B. Lorenz, P. C. W. Chu, and A. M. Guloy, Phys. Rev. B **78**, 060505 (2008).

[7] F. C. Hsu, J. Y. Luo, K. W. Yeh, T. K. Chen, T. W. Huang, P. M. Wu, Y. C. Lee, Y. L. Huang, Y. Y. Chu, D. C. Yan *et al.*, Proc. Natl. Acad. Sci. USA **105**, 14262 (2008).

[8] N. D. Zhigadlo, S. Katrych, Z. Bukowski, S. Weyeneth, R. Puzniak, and J. Karpinski, J. Phys.: Condens. Matter **20**, 342202 (2008).

[9] M. S. Z. Ban, Acta Crystallogr. **18**, 594 (1965).

[10] *Pearson's Handbook of Crystallographic Data for Intermetallic Phases*, 2nd ed, edited by P. Villars and L. D. Calvert (ASM International, Materials Park, OH, 1991).

[11] E. Colombier, S. L. Bud'ko, N. Ni, and P. C. Canfield, Phys. Rev. B **79**, 224518 (2009).

[12] R. Cortes-Gil, D. R. Parker, M. J. Pitcher, J. Hadermann, and S. J. Clarke, Chem. Mater. **22**, 4304 (2010).

[13] S. Aswartham, C. Nacke, G. Friemel, N. Leps, S. Wurmehl, N. Wizent, C. Hess, R. Klingeler, G. Behr, S. Singh *et al.*, J. Cryst. Growth **314**, 341 (2011).

[14] R. R. Urbano, E. L. Green, W. G. Moulton, A. P. Reyes, P. L. Kuhns, E. M. Bittar, C. Adriano, T. M. Garitezi, L. Bufaical, and P. G. Pagliuso, Phys. Rev. Lett. **105**, 107001 (2010).

[15] S. Avci, O. Chmaissem, E. A. Goremychkin, S. Rosenkranz, J.-P. Castellan, D. Y. Chung, I. S. Todorov, J. A. Schlueter, H. Claus, M. G. Kanatzidis *et al.*, Phys. Rev. B **83**, 172503 (2011).

[16] J. L. Mathieu and S. E. Latturner, Chem. Commun. **33**, 4965 (2009).

[17] R. Klingeler, N. Leps, I. Hellmann, A. Popa, U. Stockert, C. Hess, V. Kataev, H.-J. Grafe, F. Hammerath, G. Lang *et al.*, Phys. Rev. B **81**, 024506 (2010).

[18] X. F. Wang, T. Wu, G. Wu, H. Chen, Y. L. Xie, J. J. Ying, Y. J. Yan, R. H. Liu, and X. H. Chen, Phys. Rev. Lett. **102**, 117005 (2009).

[19]B. Shen, H. Yang, Z.-S. Wang, F. Han, B. Zeng, L. Shan, C. Ren, and H.-H. Wen, Phys. Rev. B **84**, 184512 (2011).
[20]L. Fang, H. Luo, P. Cheng, Z. Wang, Y. Jia, G. Mu, B. Shen, I. I. Mazin, L. Shan, C. Ren *et al*., Phys. Rev. B **80**, 140508 (2009).
[21]F. Rullier-Albenque, D. Colson, A. Forget, and H. Alloul, Phys. Rev. Lett. **103**, 057001 (2009).
[22]N. Ni, M. E. Tillman, J.-Q. Yan, A. Kracher, S. T. Hannahs, S. L. Bud'ko, and P. C. Canfield, Phys. Rev. B **78**, 214515 (2008).
[23]L. Harnagea, S. Singh, G. Friemel, N. Leps, D. Bombor, M. Abdel-Hafiez, A. U. B. Wolter, C. Hess, R. Klingeler, G. Behr *et al*., Phys. Rev. B **83**, 094523 (2011).
[24]M. Rotter, M. Tegel, D. Johrendt, I. Schellenberg, W. Hermes, and R. Pöttgen, Phys. Rev. B **78**, 020503 (2008).
[25]A. S. Sefat, M. A. McGuire, R. Jin, B. C. Sales, D. Mandrus, F. Ronning, E. D. Bauer, and Y. Mozharivskyj, Phys. Rev. B **79**, 094508 (2009).
[26]C. Kant, J. Deisenhofer, A. Günther, F. Schrettle, A. Loidl, M. Rotter, and D. Johrendt, Phys. Rev. B **81**, 014529 (2010).
[27]K. Zhao, Q. Q. Liu, X. C. Wang, Z. Deng, Y. X. Lv, J. L. Zhu, F. Y. Li, and C. Q. Jin, Phys. Rev. B **84**, 184534 (2011).
[28]U. Welp, R. Xie, A. E. Koshelev, W. K. Kwok, H. Q. Luo, Z. S. Wang, G. Mu, and H. H. Wen, Phys. Rev. B **79**, 094505 (2009).
[29]G. Mu, H. Luo, Z. Wang, L. Shan, C. Ren, and H. H. Wen, Phys. Rev. B **79**, 174501 (2009).
[30]A. K. Pramanik, M. Abdel-Hafiez, S. Aswartham, A. U. B. Wolter, S. Wurmehl, V. Kataev, and B. Büchner, Phys. Rev. B **84**, 064525 (2011).
[31]R. F. J.E. Gordon, M. L. Tan, and N. Phillips, Solid State Commun. **69**, 625 (1989).
[32]N. R. Werthamer, E. Helfand, and P. C. Hohenberg, Phys. Rev. **147**, 295 (1966).
[33]D. V. Evtushinsky, D. S. Inosov, V. B. Zabolotnyy, A. Koitzsch, M. Knupfer, B. Büchner, M. S. Viazovska, G. L. Sun, V. Hinkov, A. V. Boris *et al*., Phys. Rev. B **79**, 054517 (2009).
[34]V. B. Zabolotnyy, D. S. Inosov, D. V. Evtushinsky, A. Koitzsch, A. A. Kordyuk, G. L. Sun, J. T. Park, D. Haug, V. Hinkov, A. V. Boris *et al*., Nature (London) **457**, 569 (2008).